Nuclear Engineering and Design 322 (2017) 104–115

Contents lists available at ScienceDirect

Nuclear Engineering and Design

journal homepage: www.elsevier.com/locate/nucengdes

# Development and validation of a PWR on-line power-distribution monitoring system NECP-ONION

Zhuo Li [a], Liangzhi Cao [a,*], Hongchun Wu [a], Yunzhao Li [a], Zhouyu Liu [a], Wei Shen [a,b], Wen Yang [a]

[a] Xi'an Jiaotong University, Xi'an, Shaanxi, China
[b] Canadian Nuclear Safety Commission, Ottawa, Ontario, Canada

## HIGHLIGHTS

- An On-line power-distribution monitoring system has been developed and validated.
- The harmonics expansion method is adopted as the major monitoring method.
- BEAVRS benchmark has been used to verify and validate the monitoring system.
- Two improvements have been studied to increase the monitoring accuracy.
- The numerical results indicate that the monitoring is accurate for BEAVRS.

## ARTICLE INFO

*Article history:*
Received 10 October 2016
Received in revised form 23 May 2017
Accepted 8 June 2017

*Keywords:*
On-line monitoring system
Harmonics expansion method
Detector failure
BEAVRS benchmark

## ABSTRACT

A 3D on-line power-distribution monitoring system NECP-ONION has been developed and validated in this paper. It includes plant data processing, core calculation and on-line power-distribution monitoring. The diagnosis and treatment of the detector failure, core state-parameter calculation and monitoring method has been investigated to address the key issues of the on-line monitoring system. Detector failure is diagnosed by comparing with average measurements and monitored responses. The fuel-burnup calculation is performed based on the macro-depletion method due to its high efficiency. The harmonics expansion method is adopted as the major monitoring method due to its long history of maturity and success. In the investigation of the harmonics expansion method, the determination of expansion orders and choice of expansion basis functions have also been studied. The on-line monitoring system NECP-ONION was verified and validated by the diffusion calculation and real detector measurements for the BEAVRS benchmark. The verification shows that, for BEAVRS cycle 1 with a complex power history, the monitoring power distributions are almost identical to the reference power distributions once the detector "measurements" are derived from the diffusion calculation. The validation shows that differences between monitored and measured ones are small for most of the burnup steps from BOC to EOC, except for a few abnormal discrepancies at specific burnup steps. Investigation shows that those discrepancies are caused by the detector failure, complex operation history, unknown control rod positions, and unidentified operation events which cannot be modeled directly in the simulation. Two improvements have been studied to increase the monitoring accuracy of the NECP-ONION system. The numerical results indicate that these two improvements are useful to increase the monitoring accuracy for the BEAVRS benchmark.



## 1. Introduction

On-line monitoring of 3D power distribution is one of the most important technologies for a nuclear reactor. Firstly, 3D power distribution is one of the most direct responses for reactor core safety but it changes complexly. Secondly, on-line power-distribution monitoring can be employed to reduce the over-conservative operating principles (Luo et al., 2000) and hence improve the economy of nuclear power plants (Peng et al., 2014). Thirdly, on-line power-distribution monitoring provides useful information for the core calculation and safety-margin calculation.

Usually, on-line power-distribution monitoring is based upon a number of neutron-detector measurements at strategically

* Corresponding author at: No. 28 Xianning West Road, Xi'an, Shaanxi 710049, China.
E-mail address: caolz@mail.xjtu.edu.cn (L. Cao).

http://dx.doi.org/10.1016/j.nucengdes.2017.06.016
0029-5493/

selected locations in or out of the core. Since the number of detectors is limited, the locations of the detectors are separated. The main goal of the on-line power-distribution monitoring system is to estimate the spatially continuous power distribution from the real-time discrete measurements.

Several power distribution monitoring methods, such as harmonics expansion method (Li, 1994), simulation and correction method (Beard and Morita, 1988), internal boundary condition method (Chan and Mamourian, 1990), coupling coefficients method (Terney et al., 1983) and least squares method (Lee and Kim, 2003), have been developed in the past decades.

Harmonics expansion method, also called modal expansion method, time synthesis approximation or flux synthesis method, is the earliest one developed by AECL (Hinchley and Kugler, 1974; Shen and Schwanke, 2012). Its initial purpose was to calibrate zone-control-detectors by providing average zone fluxes for on-line spatial power control. In this method, reactor-core power distribution is expanded by harmonics, which are high-order eigenvectors of the neutron-diffusion equation. Detector measurements are used to determine the expansion coefficients. For CANDU reactors, this method has been in use for about 40 years. Accordingly, if the expanded function is the error of calculated power distribution instead of the power distribution, it becomes error-shape synthesis method (Hong, 2004). Simulation and correction method, adopted in BEACON (Beard and Morita, 1988) of Westinghouse, is another method used by the LWR industry. According to the core state parameters, the neutron-diffusion equation is solved to obtain the core-power distribution and the detector "measurements", called predicted or calculated values. What follows is to fit the ratios of detector measured values over predicted values to obtain a spatially continuous proportion function defined through the entire core. Finally, the monitoring result of power distribution can be obtained by multiplying the proportion function to the predicted power distribution. For the internal boundary condition method, proposed by Chan (Chan and Mamourian, 1990), the neutron-diffusion equation and detector measurements are combined by solving the neutron-diffusion equation directly using the measurements as internal boundary conditions. It was improved by introducing Kalman filtering technique to reduce calculation and measurement errors (Jeong and Cho, 2000). Similarly, in the least square method (Hong et al., 2005), the neutron-diffusion equation is coupled with the detector-response equation representing the relationship between neutron fluxes and detector signals on the least square principle. Coupling coefficients method, also named CECOR method, estimates power distributions with pre-calculated coupling coefficients from the neutron-diffusion equation and detector measurements (Jeong et al., 2014).

The neutron-diffusion equation shows relationship of local powers at different position in a core; the detector measurement shows the real-time behavior. On-line monitoring methods combine the neutron-diffusion equation and neutron-detector measurements to achieve the estimation of power distribution from discrete to continuous. Besides monitoring method, there are also other important elements in an on-line power-distribution monitoring system.

In PWR the in-core fixed detector such as self-powered neutron detector (SPND) is widely used in the monitoring system due to its accuracy compared with the ex-core fixed detector and the real-time character compared with the in-core movable detector. The SPND is constituted by three main parts, an emitter, a collector and an insulation. After the emitter captures neutrons and produces electrons, the collector collects electrons to generate electric current providing a measurable signal. This signal is transferred through an amplifier and a lead cable to plant computers. Hence, in an on-line monitoring system, the detector-measured signals are electric signals, and the amplitudes of which are directly related to the detector material (such as the neutron-capture cross section, electron-emission reaction, etc.) and the electrical element. Consequently, attentions should be paid for the following key issues:

(1) The determination of relationship between the electric current signal and the reactor core flux/power (usually called detector measurement). This relationship would be significantly affected by the location of the detector and the material of the detector emitter, which means the same signal may refer to different flux/power values.
(2) The depletion of the detector emitter. On the one hand, since detector emitter produces electrons by capturing neutrons, its cross section of neutron capture determines its sensitivity. On the other hand, the bigger its cross section is, the faster it depletes. In fact, the depletion of the detector emitter is one of the main constraints for a detector's life.
(3) Detector response time. As electrons production takes time, there is a delay of the detector signal which will lead to a delay in the response of the on-line monitoring system (Mishra et al., 2014).
(4) The diagnosis and treatment of the detector failure. Taking CANDU6 as an example, the detector failure causes the degradation of setbacks on zone powers and unnecessary spatial control actions. Consequently, on-line monitoring system should have a built-in feature to produce reliable results even after the failure of certain number of detectors. Traditionally, there is usually one special parameter together with the measured value indicating whether the detector signal is good enough. But this parameter expresses more about whether the electronic elements are working or not. Nowadays, neutronics analysis performs the diagnosis for the detector failure by comparing the monitored and measured values. A detector failure is confirmed when the difference between these two is larger than an acceptance criteria or the measured value is obviously out of range.

Besides detector measurements, the on-line power-distribution monitoring system also requires core state parameters, including control rod positions, boron concentration, coolant inlet temperature, core-average burnup and fuel-assembly burnup for the pre-simulations. The first three state parameters listed above can be measured directly during the reactor operation. But the core-average burnup and fuel-assembly burnup are unmeasurable parameters and they can only be estimated by the on-line power-distribution monitoring system. It is faster to use the pre-calculated history condition to estimate the current fuel burnup, while it is more accurate to calculate the fuel burnup step-by-step according to the most recent monitoring results based on the real history condition.

Considering the fact that on-line monitoring results can be closely related to the reactor safety, confidence on the monitored results should be guaranteed, which makes the uncertainty analysis important to evaluate the on-line monitoring method and to reduce the synthesis uncertainty. There are several uncertainty sources in the on-line monitoring system, including the modeling uncertainty and input-parameter uncertainty. The detector-measurement uncertainty is the main contribution to on-line power-distribution monitoring uncertainty as the detector measurements are strongly influenced by industrial factors and sometimes they may even be failed.

In responding to the above-mentioned key issues of on-line monitoring system, the diagnosis and treatment of the detector failure, core calculation, and monitoring method have been investigated in this paper. A 3D on-line monitoring system named

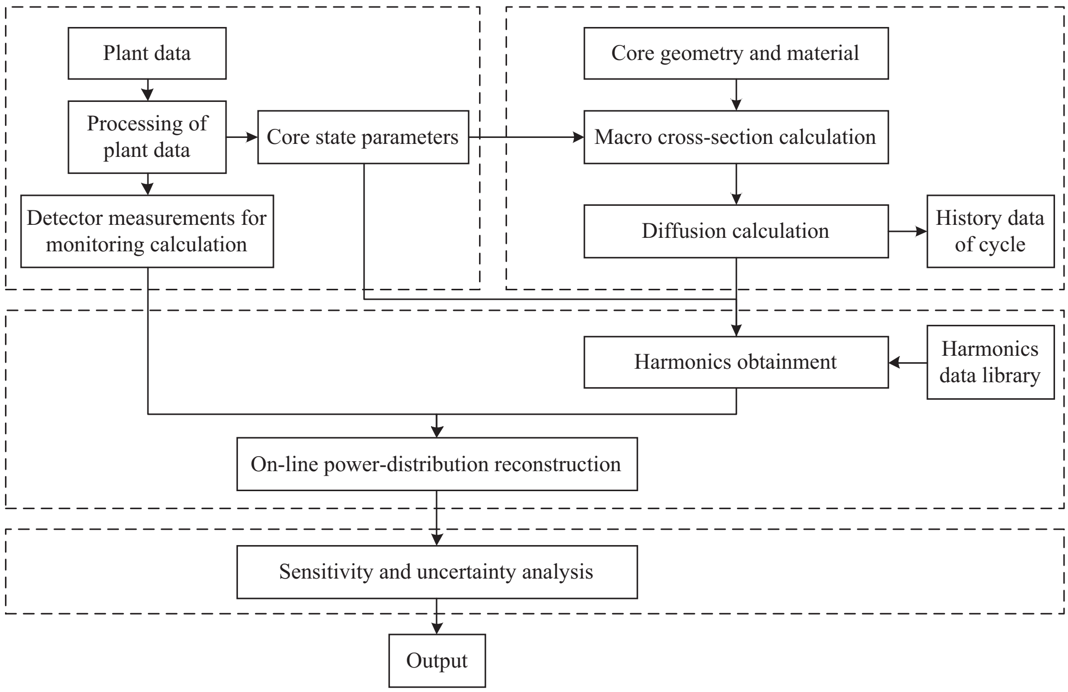


**Fig. 1.** Flow chart of the on-line monitoring system NECP-ONION.

NECP-ONION has been developed (Li et al., 2015) based on the harmonics expansion method. The harmonics expansion method is adopted as the major monitoring method due to its long history of maturity and success. The fuel-burnup calculation is performed based on the macro-depletion method. The on-line monitoring system NECP-ONION was verified and validated by the diffusion calculation and real detector measurements for the BEAVRS benchmark.

The rest of this paper is organized as follows. Section 2 describes the on-line monitoring system NECP-ONION and associated monitoring method. Verification and validation results are given in Section 3. Conclusions are summarized in Section 4.

## 2. Method

### 2.1. On-line power-distribution monitoring system

There are four steps in an integrated 3D on-line power-distribution monitoring system. The first step is reading measured plant data, transmitting and processing of data, and performing detector failure diagnosis. The second step is performing numerical simulations including core state-parameter calculation, assembly cross-section calculation, power-distribution and burnup-distribution calculations, and detector material depletion calculation. The third step is performing on-line power-distribution reconstruction by the monitoring method. The last step is the sensitivity and uncertainty analysis. Flow chart of the on-line monitoring system NECP-ONION is shown in Fig. 1.

Note that different time steps are used in the system for different modules as shown in Fig. 2, in which, $\Delta t_c$ is the time step for the diffusion calculation. This time step depends on the change of the core state which does not change significantly in minutes. So this time step can be set to be 10–30 min. $\Delta t_r$ is the time step for on-line power-distribution reconstruction calculation. This time step is decided by the requirement of monitoring results and it is usually set to be 30 s–2 min. $\Delta t_m$ is the time step for the plant data processing. This time step depends on detector's responding character and it is suggested to be 10–20 s.

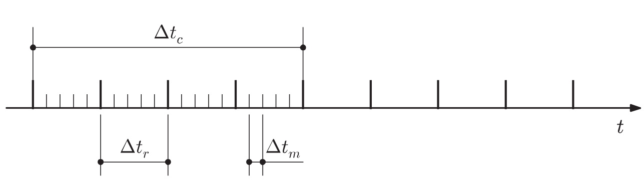


**Fig. 2.** Time steps for the on-line monitoring system.

### 2.2. Processing of plant data

Data read from plant in this part includes not only detector signals but also parts of core state parameters. Flow chart of reading and processing plant data is shown in Fig. 3.

The relationship between detector readings (electric current) and neutron fluxes can be written as Eq. (1).

$$I(r_d) = C_d N_d \sum_{g=1}^{G} \left(\sigma_g(r_d) \cdot \Phi_g(r_d)\right) \tag{1}$$

where, $I$ is electric current; $r_d$ is detector position; $C_d$ is correction coefficient of detector at $r_d$; $N_d$ is the number density of detector sensitivity material; $g$ is energy group, $g = 1, \ldots, G$; $\sigma_g(r_d)$ is capture cross section of group $g$ of detector at $r_d$; $\Phi_g(r_d)$ is neutron flux of group $g$ at position $r_d$.

Detector electric signals are affected by sensitivity of detectors, electric elements and cable, and background signals. These effects are all represented by correction coefficient $C_d$. In this paper, the coefficients are assumed to be known when monitoring calculation is carried out. Neutron fluxes are calculated by diffusion equation and are on-line reconstructed.

Flow chart about detector failure is shown in Fig. 4. The preliminary diagnosis is just for measurements. When zero or negative value appeared, detector failure is considered. Compared with other measurements, detectors with values $m$ times larger or smaller than average measurements are considered failed. In addition, diagnosis is processed with monitoring calculation by comparing detector measurements with reconstructed detector responses. Detector failure is determined when errors between measured

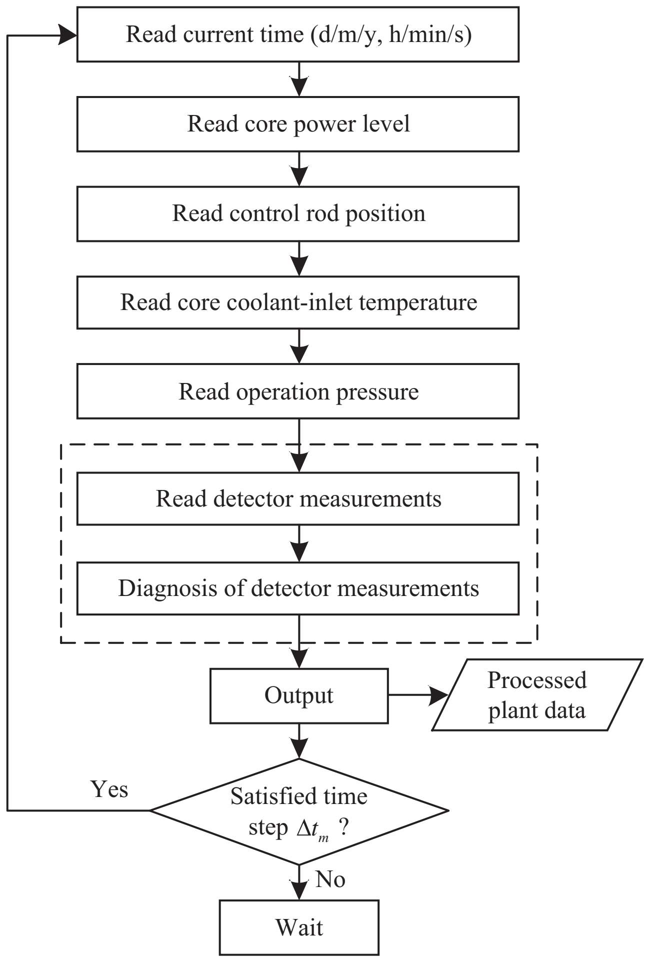


**Fig. 3.** Flow chart of the plant-data processing.

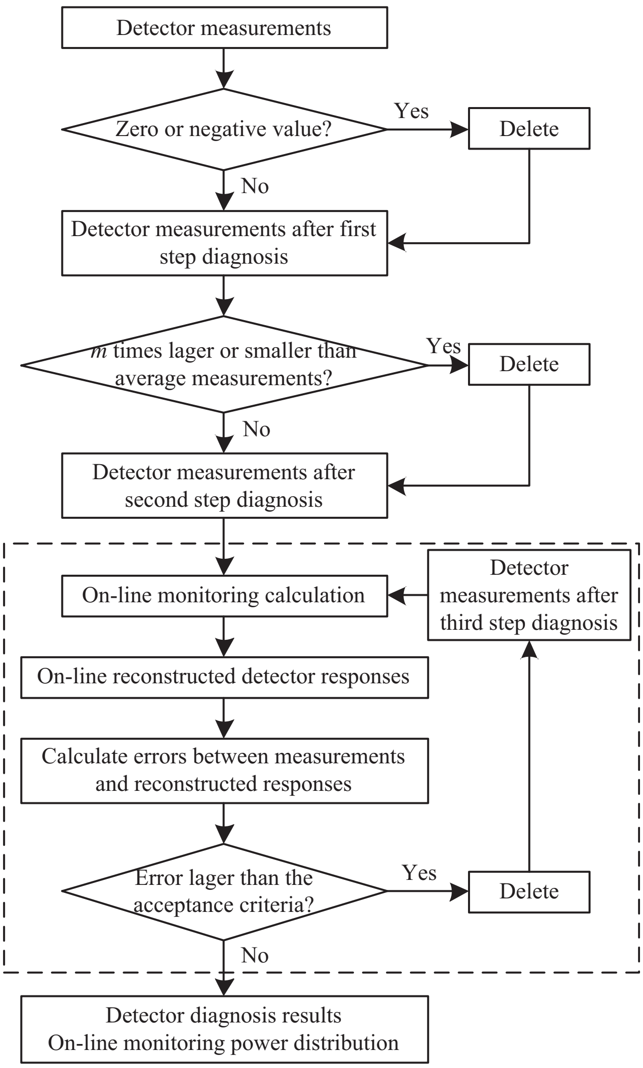


**Fig. 4.** Flow chart of the detector failure diagnosis.

and reconstructed detector responses are larger than the acceptance criteria. This comparison combines measurements of rounded and symmetric detectors to determine if failure happens.

### 2.3. Core calculation

Core calculation includes power-distribution calculation, burnup-distribution calculation, and detector responses prediction calculation. Flow chart of this part is shown in Fig. 5.

In the on-line monitoring system, one certain burnup time-step first reads last step information, including the burnup distribution. Based on the core state parameters, assembly macro cross sections can be generated for the diffusion calculation. After that, power distribution and assembly burnup distribution would be updated with the diffusion solution. The power distribution would be used as the convergence criteria for burnup and power distribution calculation. The next time step will then use the new burnup distribution to generate macro cross sections.

In the harmonics expansion method, the core-average burnup level is used to calculate harmonics from the harmonics library, with the given boron concentration and control rod position. The burnup distribution can be used to generate assembly cross sections.

The increment of the core-average burnup is calculated via the operation power history and the core heavy metal loading pattern by,

$$\Delta Bu^k_{\mathrm{Core}} = \frac{P^k_{\mathrm{Core}} \cdot \Delta t^k}{G_{\mathrm{Core}}} \tag{2}$$

where, $\Delta Bu^k_{\mathrm{Core}}$ is the increment of the core-average burnup in the operation time $\Delta t^k$. $P^k_{\mathrm{Core}}$ is the core operation power in the operation time $\Delta t^k$; $G_{Core}$ is total heavy metal loading in the core.

Similarly, the increment of the fuel-assembly burnup is calculated by,

$$\Delta Bu^k_{\mathrm{Assembly}}(r_i) = \frac{P^k_{\mathrm{Assembly}}(r_i) \cdot \Delta t^k}{G_{\mathrm{Assembly}}(r_i)} \tag{3}$$

where, $\Delta Bu^k_{\mathrm{Assembly}}(r_i)$ is the increment of assembly burnup in the operation time $\Delta t^k$; $r_i$ is the assembly position in the core; $P^k_{\mathrm{Assembly}}(r_i)$ is the assembly power during the time interval $\Delta t^k$; $G_{\mathrm{Assembly}}(r_i)$ is the heavy metal loading in the assembly.

### 2.4. Monitoring method

The definition of harmonics is based on the neutron-diffusion equation which can be written in operator form as below:

$$M\Phi = \frac{1}{k} F\Phi \tag{4}$$

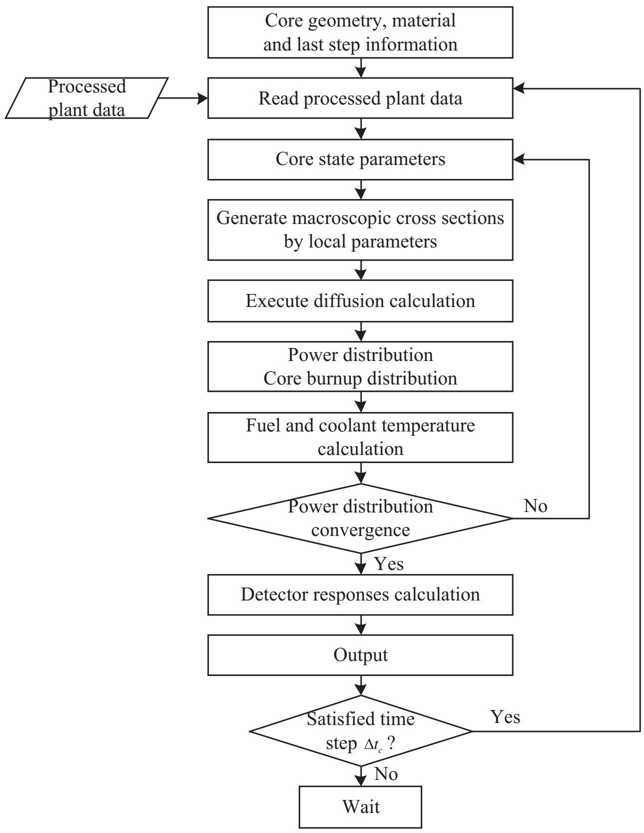


**Fig. 5.** Flow chart of the core calculation.

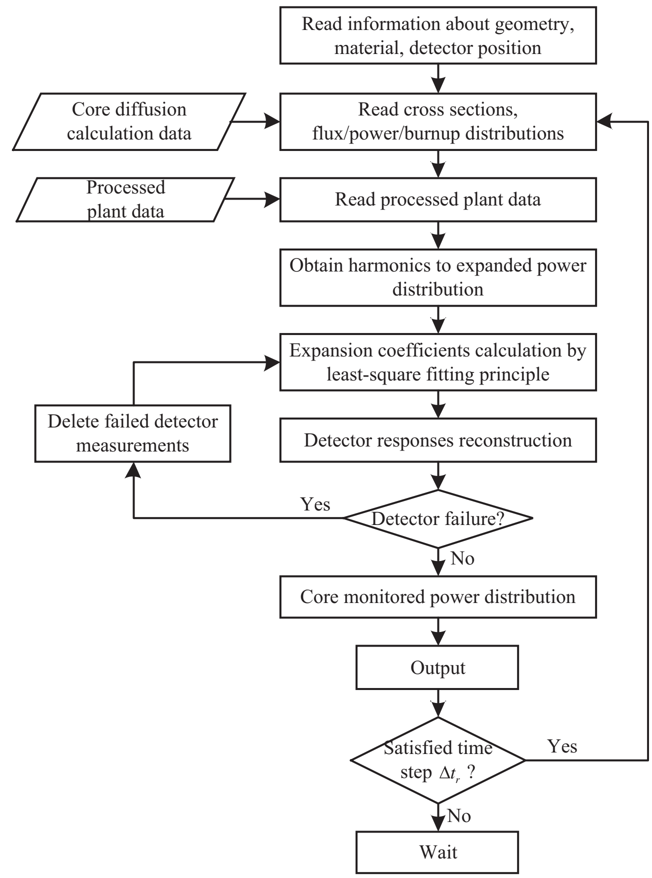


**Fig. 6.** Flow chart of the monitoring calculation.

where, $M$ and $F$ are neutron destruction and generation operators; $\Phi$ is neutron flux; $k$ is effective multiplication factor.

Define operator $A = M^{-1}F$, then neutron-diffusion equation can be written as follow:

$$A\Phi = k\Phi \tag{5}$$

This is an eigenvalue equation which has serial eigenvalues and corresponding eigenvectors. These eigenvectors are called harmonics. Especially, the first-order harmonic, also called as basic or fundamental mode, is the neutron-flux distribution. $k_1$ is the effective multiplication factor.

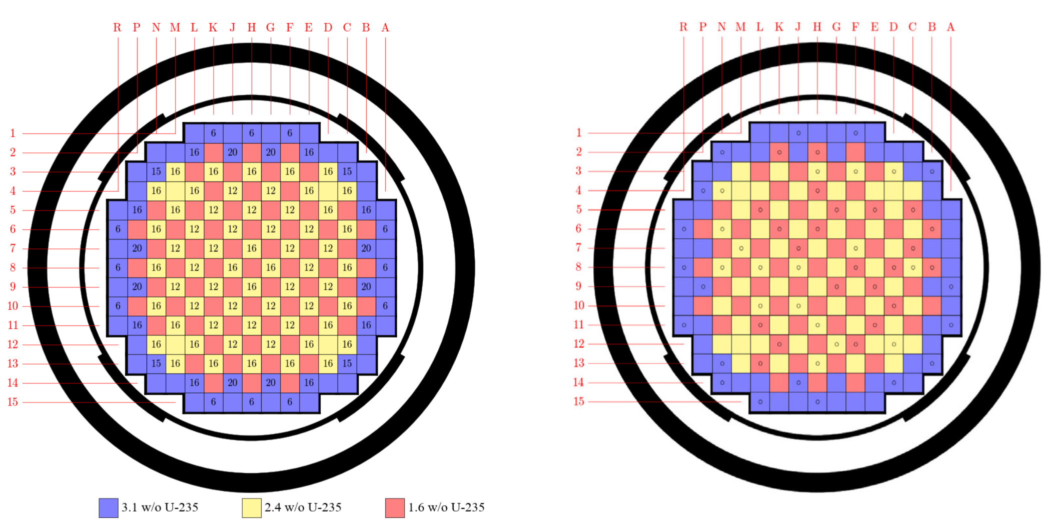


(a) Layout of fuel assemblies and BPs positions

(b) Instrumentation tube positions

**Fig. 7.** Layout of fuel assemblies, burnable poison positions and instrumentation tube positions in cycle 1 (Horelik and Herman, 2013). (a) Layout of fuel assemblies and BPs positions. (b) Instrumentation tube positions.

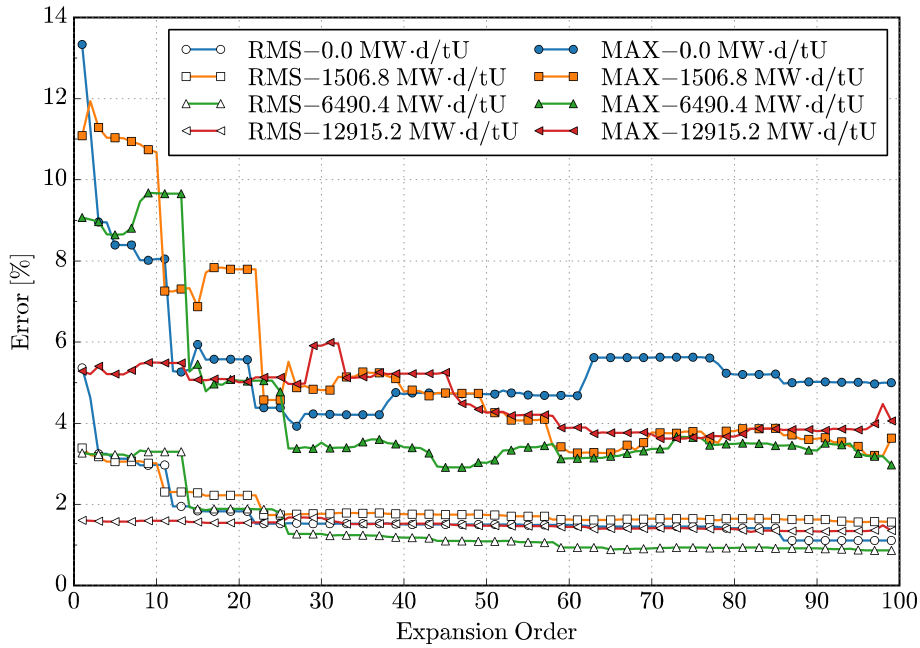


**Fig. 8.** Relative errors of radial average detector responses at different burnup levels.

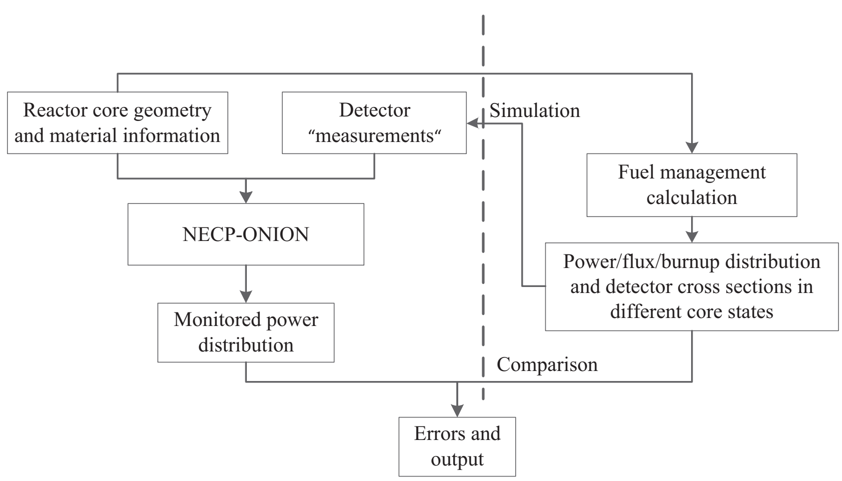


**Fig. 9.** Flow chart of comparison with diffusion calculation.

It has been proved that harmonics compose a set of complete basis functions (Li et al., 1997). Taking two-group approximation as an example, power distribution can be expanded by harmonics:

$$P(r) = \kappa\Sigma_{f1}(r)\sum_{n=1}^{N} a_n \Phi_{1,n}(r) + \kappa\Sigma_{f2}(r)\sum_{n=1}^{N} b_n \Phi_{2,n}(r) \quad (6)$$

where, $P(r)$ is the expanded power distribution; $r$ is the spatial variable; $\kappa\Sigma_{f1}$ and $\kappa\Sigma_{f2}$ are cross sections; $N$ is the number of harmonics; $a_n$ and $b_n$ are the $n$th-order expansion coefficients.

The expansion coefficients are solved by detector measurements.

$$I(r_d) = C_d N_d \left(\sigma_1(r_d)\sum_{n=1}^{N} a_n \Phi_{1,n}(r_d) + \sigma_2(r_d)\sum_{n=1}^{N} b_n \Phi_{2,n}(r_d)\right) \quad (7)$$

If the number of detectors is $M_d$, a set of equations can be obtained as follows:

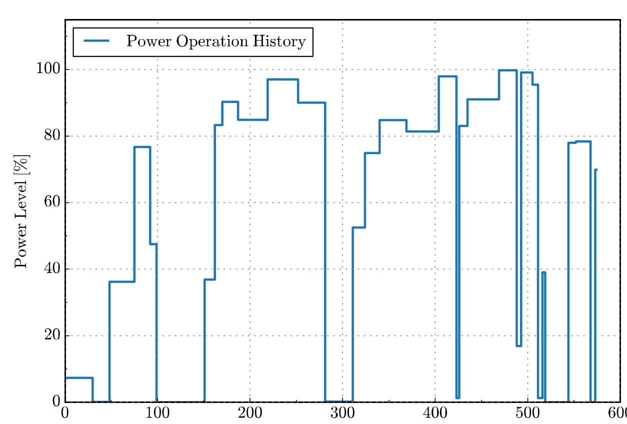


**Fig. 10.** Power operation history for reference calculation by NECP-CYPRESS.

$$\begin{cases} I(r_1) = C_1 N_1 \left( \sigma_1(r_1) \sum_{n=1}^{N} a_n \Phi_{1,n}(r_1) + \sigma_2(r_1) \sum_{n=1}^{N} b_n \Phi_{2,n}(r_1) \right) \\ I(r_2) = C_2 N_2 \left( \sigma_1(r_2) \sum_{n=1}^{N} a_n \Phi_{1,n}(r_2) + \sigma_2(r_2) \sum_{n=1}^{N} b_n \Phi_{2,n}(r_2) \right) \\ \cdots\cdots \\ I(r_{M_d}) = C_M N_M \left( \sigma_1(r_{M_d}) \sum_{n=1}^{N} a_n \Phi_{1,n}(r_{M_d}) + \sigma_2(r_{M_d}) \sum_{n=1}^{N} b_n \Phi_{2,n}(r_{M_d}) \right) \end{cases} \tag{8}$$

Usually, detector number $M_d$ is larger than expansion order $N$. The least-square fitting method has been used for the coefficients calculation.

Krylov subspace method (Verdu et al., 1999), combined with nonlinear iteration semi-analytic nodal method (NLSANM) (Liao, 2002), has been used to solve harmonics. Krylov subspace method is widely used in recent years to solve large-matrix-eigenvalue problems for its attractive efficiency (Zinzani et al., 2008). The open-source mathematical toolkit "ARPACK" (Lehoucq et al., 1997) has been integrated in NECP-ONION for harmonics solution.

Harmonics expansion method is one kind of the expansion methods. Within which, there are two key problems. One is how to determine the number of expansion order. Though the expansion number is infinite theoretically, a certain order has to be chosen for practical use. Several problems have been tested with expansion order varying from 1 to 99 to determine a reasonable expansion order by analyzing the monitoring errors. The other one is how to choose the expansion basis functions. Harmonics data library is proposed in Wang et al. (2011) to compromise the calculation burden and accuracy. The following study shows that harmonics data library could not capture the actual operation history of the monitored core. As a result, expansion basis functions are real-time updated to improve monitoring accuracy. The nodal method combined with the Krylov subspace method makes it possible to update harmonics in real time. Flow chart for monitoring calculation is shown in Fig. 6.

## 3. Results

Based on above theories, a 3D on-line power-distribution monitoring system called NECP-ONION has been developed. The flow chart is shown in Fig. 1. It reads and pre-processes plant data, calculates core burnup distribution, obtains harmonics and monitors power distribution on-line. Validation for each module has been performed. Detailed description about validation of detector failure, core diffusion calculation and monitoring module are listed in Refs. Li et al. (2016a), (2016b) and Li et al. (2016c), respectively.

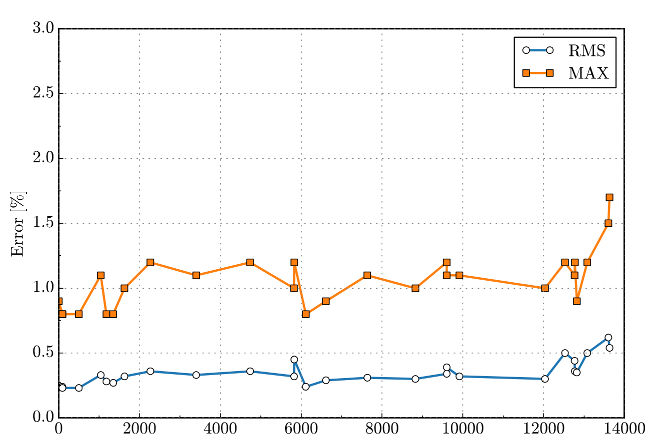


**Fig. 11.** Relative errors of radial power distributions from BOC to EOC.

Validation for the integral monitoring system is studied in this paper.

### 3.1. Problem description

Verification and validation of on-line monitoring system NECP-ONION were performed with the BEAVRS benchmark (Horelik et al., 2013) which was proposed by MIT Computational Reactor

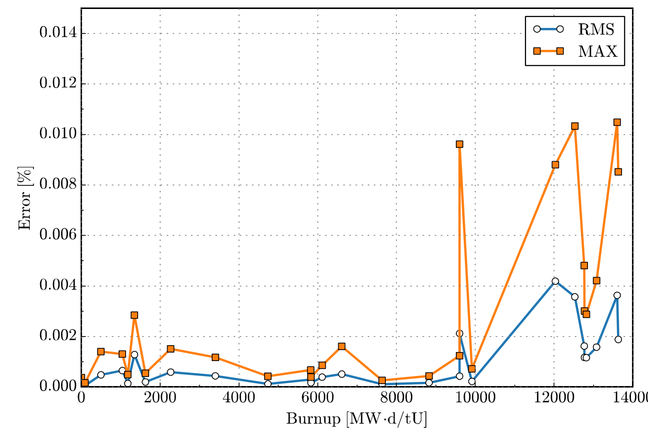


**Fig. 12.** Relative errors of radial power distributions from BOC to EOC (Update first-order harmonic by NECP-CYPRESS).

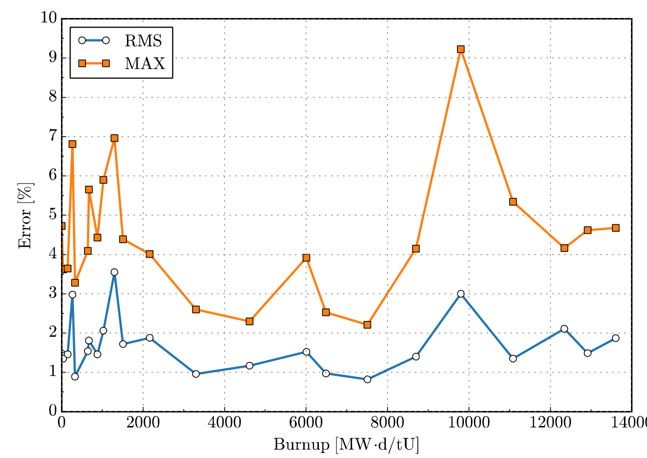


**Fig. 13.** Relative errors of radial-average detector responses of cycle 1.

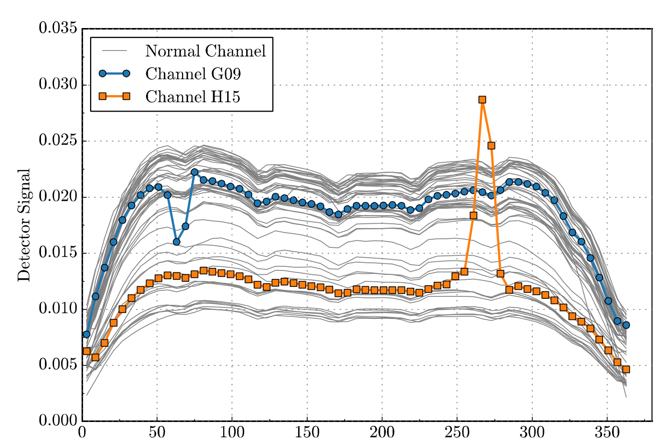


**Fig. 14.** Detector signals for 9802.9 MWd/tU.

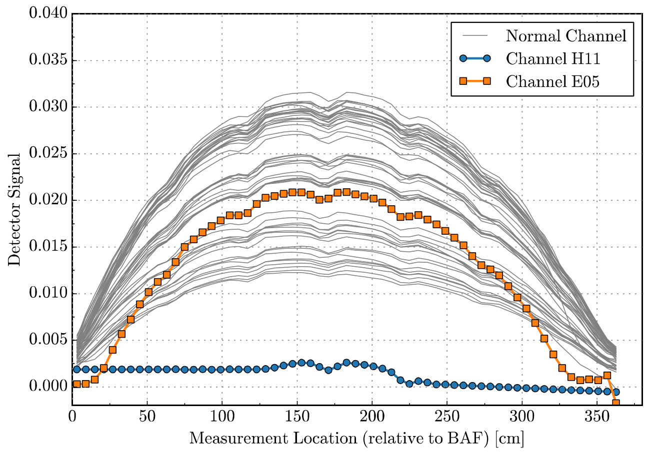


**Fig. 15.** Detector signals for 326.5 MWd/tU.

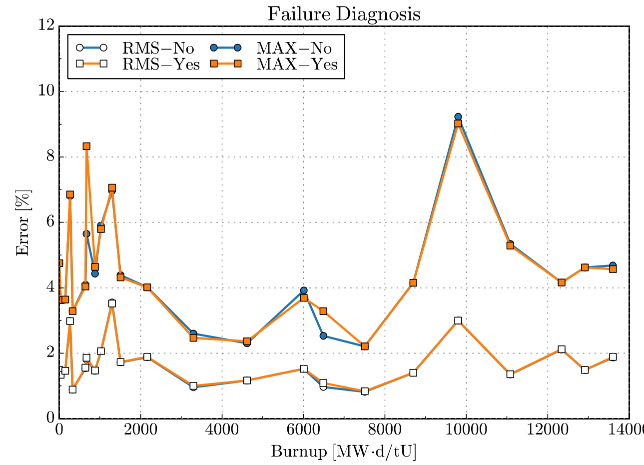


**Fig. 16.** Relative errors of radial-average detector responses with detector failure diagnosis.

Physics Group (CRPG) for the qualification of the PWR full-core calculation (Horelik and Herman, 2013). It contains detailed description about a PWR core, including geometry and material, and operation data, including measured in-core detector data, power history and critical boron concentration.

Assembly layout and burnable poison (BP) positions in cycle 1 are shown in Fig. 7a. The core power is 3411 MWth with 193 assemblies. Three enrichments are included in cycle 1, 1.6%, 2.4%

Burnup Distribution [MWd/tU]
Error [%]

| | | | | | | | | | | | | | | |
|---|---|---|---|---|---|---|---|---|---|---|---|---|---|---|
| | | | | 0.55 | 0.64 | 0.70 | 0.67 | 0.70 | 0.64 | 0.55 | | | | |
| | | | | -1.69 | -1.02 | -0.45 | 0.28 | 0.86 | 1.16 | 0.79 | | | | |
| | | 0.62 | 0.82 | 0.78 | 0.64 | 0.75 | 0.64 | 0.75 | 0.64 | 0.78 | 0.82 | 0.62 | | |
| | | -2.41 | -2.14 | -1.74 | -1.29 | -0.66 | -0.05 | 0.54 | 0.67 | 0.44 | -0.19 | -0.85 | | |
| | 0.62 | 0.83 | 0.78 | 0.70 | 0.70 | 0.64 | 0.68 | 0.64 | 0.70 | 0.70 | 0.78 | 0.83 | 0.62 | |
| | -2.38 | -1.96 | -1.98 | -2.12 | -1.69 | -1.31 | -0.58 | -0.25 | 0.04 | -0.24 | -0.22 | -0.58 | -1.33 | |
| | 0.82 | 0.78 | 0.96 | 0.75 | 0.66 | 0.73 | 0.64 | 0.73 | 0.66 | 0.75 | 0.96 | 0.78 | 0.82 | |
| | -2.08 | -1.91 | -2.43 | -2.23 | -2.24 | -1.78 | -1.40 | -0.91 | -0.73 | -0.54 | -0.89 | -0.65 | -1.04 | |
| 0.55 | 0.78 | 0.70 | 0.75 | 0.69 | 0.74 | 0.65 | 0.72 | 0.65 | 0.74 | 0.69 | 0.75 | 0.70 | 0.78 | 0.55 |
| -1.68 | -1.76 | -2.15 | -2.22 | -2.52 | -2.54 | -2.39 | -2.02 | -1.70 | -1.27 | -1.08 | -0.78 | -0.84 | -0.51 | -0.36 |
| 0.64 | 0.64 | 0.70 | 0.66 | 0.74 | 0.65 | 0.71 | 0.62 | 0.71 | 0.65 | 0.74 | 0.66 | 0.70 | 0.64 | 0.64 |
| -1.21 | -1.50 | -1.76 | -2.26 | -2.48 | -2.77 | -2.70 | -2.49 | -2.10 | -1.79 | -1.29 | -0.95 | -0.30 | 0.14 | 0.60 |
| 0.70 | 0.75 | 0.64 | 0.73 | 0.65 | 0.71 | 0.60 | 0.62 | 0.60 | 0.71 | 0.65 | 0.73 | 0.64 | 0.75 | 0.70 |
| -0.95 | -1.04 | -1.55 | -1.86 | -2.39 | -2.57 | -2.79 | -2.63 | -2.44 | -1.93 | -1.43 | -0.55 | 0.08 | 1.04 | 1.35 |
| 0.67 | 0.64 | 0.68 | 0.64 | 0.72 | 0.62 | 0.62 | 0.57 | 0.62 | 0.62 | 0.72 | 0.64 | 0.68 | 0.64 | 0.67 |
| -0.54 | -0.67 | -0.97 | -1.49 | -1.88 | -2.31 | -2.49 | -2.63 | -2.30 | -1.93 | -1.15 | -0.20 | 1.00 | 1.82 | 2.28 |
| 0.70 | 0.75 | 0.64 | 0.73 | 0.65 | 0.71 | 0.60 | 0.62 | 0.60 | 0.71 | 0.65 | 0.73 | 0.64 | 0.75 | 0.70 |
| -0.23 | -0.28 | -0.75 | -1.01 | -1.46 | -1.68 | -2.03 | -2.07 | -1.91 | -1.34 | -0.64 | 0.61 | 1.66 | 2.83 | 3.23 |
| 0.64 | 0.64 | 0.70 | 0.66 | 0.74 | 0.65 | 0.71 | 0.62 | 0.71 | 0.65 | 0.74 | 0.66 | 0.70 | 0.64 | 0.64 |
| 0.03 | -0.22 | -0.42 | -0.79 | -0.90 | -1.16 | -1.20 | -1.37 | -1.06 | -0.57 | 0.43 | 1.42 | 2.74 | 3.58 | 4.08 |
| 0.55 | 0.78 | 0.70 | 0.75 | 0.69 | 0.74 | 0.65 | 0.72 | 0.65 | 0.74 | 0.69 | 0.75 | 0.70 | 0.78 | 0.55 |
| -0.27 | -0.33 | -0.56 | -0.42 | -0.57 | -0.46 | -0.45 | -0.24 | 0.00 | 0.74 | 1.56 | 2.85 | 3.54 | 4.42 | 4.42 |
| | 0.82 | 0.78 | 0.96 | 0.75 | 0.66 | 0.73 | 0.64 | 0.73 | 0.66 | 0.75 | 0.96 | 0.78 | 0.82 | |
| | -0.69 | -0.34 | -0.58 | -0.08 | 0.14 | 0.62 | 0.89 | 1.45 | 1.95 | 3.09 | 3.70 | 4.82 | 4.87 | |
| | 0.62 | 0.83 | 0.78 | 0.70 | 0.70 | 0.64 | 0.68 | 0.64 | 0.70 | 0.70 | 0.78 | 0.83 | 0.62 | |
| | -1.11 | -0.44 | -0.05 | 0.11 | 0.89 | 1.50 | 2.26 | 2.67 | 3.47 | 3.96 | 4.98 | 5.45 | 5.05 | |
| | | 0.62 | 0.82 | 0.78 | 0.64 | 0.75 | 0.64 | 0.75 | 0.64 | 0.78 | 0.82 | 0.62 | | |
| | | -0.95 | -0.24 | 0.72 | 1.62 | 2.59 | 3.28 | 4.01 | 4.44 | 4.96 | 5.20 | 5.10 | | |
| | | | | 0.55 | 0.64 | 0.70 | 0.67 | 0.70 | 0.64 | 0.55 | | | | |
| | | | | 1.14 | 2.26 | 3.06 | 3.90 | 4.54 | 5.12 | 5.12 | | | | |

**Fig. 17.** Changes of burnup distribution by monitored power feedback.

and 3.1%. Fuel type is 17 × 17 with 264 fuel rods. There are two types of asymmetrical BP layout assemblies in cycle 1, with 6 and 15 BPs.

The detector tubes are shown in Fig. 7b. 58 detector tubes with 61 axial detector measurements are provided by BEAVRS benchmark. These measurements are obtained by in-core moveable detectors measuring about once per month when reactor is in normal operation condition. In practical application, monitoring system uses real-time in-core fixed detector measurements. In this paper, on-line monitoring calculation uses the moveable-detector measurements as inputs.

### 3.2. Expansion order determination

Different expansion order from 1 to 99 has been studied for BEAVRS benchmark with different burnup, for hot zero power, beginning of cycle (BOC), middle of cycle (MOC) and end of cycle (EOC). The measurements provided by benchmark are taken as references. The relative errors of radial-average detector responses are shown in Fig. 8, including root-mean-square errors (RMS) and maximum errors (MAX). It is clearly depicted in Fig. 8 that when expansion order equals 1, the monitoring error is equivalent to diffusion calculation error. When the expansion order increases from 1 to 30, the monitoring errors are decreased significantly for all the burnup levels. But when the expansion order is larger than 30, the RMS errors only decreases slightly. Considering the RMS errors and MAX errors comprehensively, an order of 50 is chosen for BEAVRS benchmark monitoring calculation.

### 3.3. Verification

Before comparing with the plant measurements, the primary verification for NECP-ONION was carried out by comparing with the diffusion calculation to assess the faithfulness of the on-line monitoring system against the conceptual design of the NECP-ONION system.

The flow chart of this comparison is shown in Fig. 9. It contains four steps. (1) Reference power distribution: calculate the power distribution based on the specified power operation history by the fuel management code. (2) Detector measurements: simulate detector "measurements" based on the calculated flux distribution and detector cross sections by the fuel management code. (3) On-line monitoring: on-line reconstruct the power distribution based on "measurements". (4) Monitoring error: compare monitored (reconstructed) power distribution with the reference solution.

Normalizated Power Distribution
Error [%]

| | | | | | | | | | | | | | | |
|---|---|---|---|---|---|---|---|---|---|---|---|---|---|---|
| | | | | 0.78 | 0.90 | 0.98 | 0.95 | 0.98 | 0.90 | 0.78 | | | | |
| | | | | 1.93 | 1.74 | 1.50 | 1.23 | 0.98 | 0.78 | 0.65 | | | | |
| | | 0.86 | 1.13 | 1.09 | 0.91 | 1.07 | 0.92 | 1.07 | 0.91 | 1.09 | 1.13 | 0.86 | | |
| | | 2.18 | 2.11 | 1.97 | 1.78 | 1.53 | 1.26 | 1.00 | 0.79 | 0.63 | 0.52 | 0.45 | | |
| | 0.86 | 1.13 | 1.09 | 0.99 | 1.00 | 0.93 | 0.98 | 0.93 | 1.00 | 0.99 | 1.09 | 1.13 | 0.86 | |
| | 2.19 | 2.16 | 2.11 | 2.01 | 1.82 | 1.58 | 1.30 | 1.04 | 0.80 | 0.61 | 0.47 | 0.37 | 0.31 | |
| | 1.13 | 1.09 | 1.34 | 1.08 | 0.96 | 1.06 | 0.95 | 1.06 | 0.96 | 1.08 | 1.34 | 1.09 | 1.13 | |
| | 2.12 | 2.11 | 2.08 | 1.99 | 1.82 | 1.59 | 1.32 | 1.04 | 0.78 | 0.55 | 0.39 | 0.25 | 0.15 | |
| 0.78 | 1.09 | 0.99 | 1.08 | 1.00 | 1.09 | 0.97 | 1.07 | 0.97 | 1.09 | 1.00 | 1.08 | 0.99 | 1.09 | 0.78 |
| 1.95 | 1.99 | 2.01 | 1.99 | 1.91 | 1.76 | 1.55 | 1.28 | 0.99 | 0.70 | 0.45 | 0.24 | 0.05 | -0.12 | -0.27 |
| 0.90 | 0.91 | 1.00 | 0.96 | 1.09 | 0.97 | 1.06 | 0.94 | 1.06 | 0.97 | 1.09 | 0.96 | 1.00 | 0.91 | 0.90 |
| 1.78 | 1.81 | 1.83 | 1.81 | 1.74 | 1.62 | 1.42 | 1.16 | 0.85 | 0.54 | 0.25 | -0.02 | -0.27 | -0.47 | -0.60 |
| 0.98 | 1.07 | 0.93 | 1.06 | 0.97 | 1.06 | 0.91 | 0.94 | 0.91 | 1.06 | 0.97 | 1.06 | 0.93 | 1.07 | 0.98 |
| 1.55 | 1.57 | 1.58 | 1.56 | 1.50 | 1.38 | 1.20 | 0.92 | 0.60 | 0.26 | -0.06 | -0.38 | -0.67 | -0.90 | -1.01 |
| 0.95 | 0.92 | 0.98 | 0.95 | 1.07 | 0.94 | 0.94 | 0.86 | 0.94 | 0.94 | 1.07 | 0.95 | 0.98 | 0.92 | 0.95 |
| 1.29 | 1.30 | 1.29 | 1.26 | 1.18 | 1.06 | 0.85 | 0.56 | 0.22 | -0.13 | -0.48 | -0.82 | -1.13 | -1.36 | -1.48 |
| 0.98 | 1.07 | 0.93 | 1.06 | 0.97 | 1.06 | 0.91 | 0.94 | 0.91 | 1.06 | 0.97 | 1.06 | 0.93 | 1.07 | 0.98 |
| 1.03 | 1.01 | 0.98 | 0.92 | 0.82 | 0.66 | 0.43 | 0.12 | -0.24 | -0.60 | -0.96 | -1.31 | -1.63 | -1.85 | -1.95 |
| 0.90 | 0.91 | 1.00 | 0.96 | 1.09 | 0.97 | 1.06 | 0.94 | 1.06 | 0.97 | 1.09 | 0.96 | 1.00 | 0.91 | 0.90 |
| 0.79 | 0.75 | 0.68 | 0.59 | 0.45 | 0.25 | -0.02 | -0.35 | -0.72 | -1.10 | -1.48 | -1.84 | -2.13 | -2.31 | -2.37 |
| 0.78 | 1.09 | 0.99 | 1.08 | 1.00 | 1.09 | 0.97 | 1.07 | 0.97 | 1.09 | 1.00 | 1.08 | 0.99 | 1.09 | 0.78 |
| 0.60 | 0.51 | 0.41 | 0.27 | 0.10 | -0.14 | -0.45 | -0.81 | -1.20 | -1.60 | -2.00 | -2.35 | -2.59 | -2.70 | -2.70 |
| | 1.13 | 1.09 | 1.34 | 1.08 | 0.96 | 1.06 | 0.95 | 1.06 | 0.96 | 1.08 | 1.34 | 1.09 | 1.13 | |
| | 0.30 | 0.19 | 0.03 | -0.20 | -0.51 | -0.87 | -1.26 | -1.66 | -2.07 | -2.45 | -2.74 | -2.92 | -3.00 | |
| | 0.86 | 1.13 | 1.09 | 0.99 | 1.00 | 0.93 | 0.98 | 0.93 | 1.00 | 0.99 | 1.09 | 1.13 | 0.86 | |
| | 0.16 | 0.01 | -0.19 | -0.47 | -0.84 | -1.25 | -1.67 | -2.08 | -2.46 | -2.79 | -3.01 | -3.14 | -3.19 | |
| | | 0.86 | 1.13 | 1.09 | 0.91 | 1.07 | 0.92 | 1.07 | 0.91 | 1.09 | 1.13 | 0.86 | | |
| | | -0.12 | -0.36 | -0.72 | -1.12 | -1.55 | -1.98 | -2.37 | -2.72 | -2.98 | -3.16 | -3.26 | | |
| | | | | 0.78 | 0.90 | 0.98 | 0.95 | 0.98 | 0.90 | 0.78 | | | | |
| | | | | -0.93 | -1.30 | -1.71 | -2.13 | -2.52 | -2.83 | -3.05 | | | | |

**Fig. 18.** Changes of power distribution by monitored power feedback.

In this paper, the fuel management code NECP-CYPRESS (Li et al., 2016b), developed by NECP lab, is used for the reference power-distribution calculation. The power operation history (Kelly et al., 2014) for the reference power-distribution calculation is shown in Fig. 10.

Firstly, basis functions are all updated on-line by solving the neutron-diffusion equation from BOC to EOC. The relative errors of radial power distributions are given in Fig. 11. From 0 MWd/tU to 13629 MWd/tU, RMS errors of monitoring power distributions are less than 0.6% compared with the reference solution. The reason for this 0.6% discrepancy is partly due to different nodal methods used in the calculation: harmonics calculation uses non-linear iteration semi-analytic nodal method and the reference power distribution is solved by variational nodal method of NECP-CYPRESS.

Secondly, NECP-CYPRESS is used to update the first-order harmonic following the monitoring calculation. Fig. 12 shows the relative errors of radial power distributions. RMS errors in Fig. 12 are all less than 0.005%. This deviation on the one hand explains that errors in Fig. 11 are only the difference between different nodal methods. On the other hand, error of $10^{-5}$ is caused by the tighter convergence criterion of reference solution than that of the monitoring calculation.

### 3.4. Validation

Comparison with detector measurements of the BEAVRS benchmark is performed for the validation of NECP-ONION. Traditional two-step method has been employed for the calculation of BEAVRS core in Ref. Li et al. (2016c). Validation of the monitoring calculation was performed for the BEAVRS benchmark from BOC to EOC of cycle 1. On-line-updated first-order harmonic is employed. Relative errors of radial-average detector responses between monitored and measured ones are small for most of the burnup steps as shown in Fig. 13. However, RMS errors and MAX errors at a few burnup steps are abnormally larger than 2% and 5% respectively. Specifically, the RMS error is 3.0% and the maximum error is 9.2% at the burnup of 9802.9 MWd/tU. To understand the reasons of the abnormal discrepancies, two possible causes were investigated.

Firstly, it is observed that the measurements fluctuate abnormally in the axial direction unexpectedly as depicted in Fig. 14 for detector measurements of 9802.9 MWd/tU. This phenomenon might be caused by the detector failure.

However, considering the procedure of moveable in-core detector when measured, detectors are inserted into the core through instrumentation tubes in assemblies until the top of the assembly

Monitored Detector Response
Error [%]

| | | | | | | | | | | | | | | |
|---|---|---|---|---|---|---|---|---|---|---|---|---|---|---|
| | | | | 0.56 | 0.70 | 0.78 | 0.77 | 0.78 | 0.71 | 0.57 | | | | |
| | | | | 0.17 | 0.01 | -0.09 | -0.09 | -0.05 | 0.08 | 0.26 | | | | |
| | | 0.61 | 0.81 | 0.84 | 1.22 | 0.85 | 1.28 | 0.86 | 1.23 | 0.86 | 0.82 | 0.61 | | |
| | | 0.09 | -0.02 | -0.01 | 0.02 | -0.06 | -0.04 | -0.02 | 0.08 | 0.07 | 0.05 | 0.17 | | |
| | 0.61 | 0.73 | 1.04 | 1.25 | 0.95 | 1.21 | 0.97 | 1.22 | 0.96 | 1.27 | 1.06 | 0.74 | 0.62 | |
| | 0.12 | -0.04 | -0.13 | -0.04 | 0.02 | 0.03 | 0.02 | 0.06 | 0.07 | 0.02 | -0.06 | 0.02 | 0.18 | |
| | 0.81 | 1.05 | 1.17 | 1.00 | 1.20 | 0.99 | 1.21 | 1.00 | 1.22 | 1.02 | 1.19 | 1.06 | 0.83 | |
| | 0.03 | -0.10 | -0.22 | -0.08 | 0.01 | 0.01 | 0.03 | 0.03 | 0.05 | -0.03 | -0.17 | -0.05 | 0.08 | |
| 0.56 | 0.85 | 1.25 | 1.00 | 1.23 | 0.99 | 1.21 | 0.99 | 1.22 | 1.01 | 1.25 | 1.02 | 1.28 | 0.87 | 0.58 |
| 0.24 | 0.05 | -0.01 | -0.07 | -0.04 | -0.03 | 0.00 | -0.01 | 0.01 | 0.01 | -0.01 | -0.02 | 0.04 | 0.10 | 0.29 |
| 0.70 | 1.22 | 0.95 | 1.20 | 0.99 | 1.20 | 0.97 | 1.17 | 0.97 | 1.22 | 1.01 | 1.23 | 0.98 | 1.25 | 0.73 |
| 0.06 | 0.06 | 0.05 | 0.03 | -0.02 | -0.02 | -0.03 | 0.00 | -0.01 | 0.00 | 0.01 | 0.07 | 0.10 | 0.11 | 0.11 |
| 0.77 | 0.85 | 1.21 | 0.99 | 1.21 | 0.97 | 1.13 | 0.87 | 1.13 | 0.98 | 1.23 | 1.01 | 1.24 | 0.88 | 0.80 |
| -0.08 | -0.04 | 0.04 | 0.02 | 0.00 | -0.02 | 0.01 | 0.02 | 0.02 | 0.00 | 0.03 | 0.06 | 0.08 | 0.01 | -0.02 |
| 0.76 | 1.26 | 0.96 | 1.21 | 0.99 | 1.17 | 0.87 | 1.07 | 0.88 | 1.18 | 1.00 | 1.23 | 0.98 | 1.30 | 0.79 |
| -0.12 | -0.07 | 0.01 | 0.03 | -0.01 | 0.00 | 0.03 | 0.06 | 0.03 | 0.02 | 0.01 | 0.06 | 0.05 | -0.02 | -0.06 |
| 0.77 | 0.85 | 1.22 | 1.00 | 1.22 | 0.98 | 1.14 | 0.88 | 1.14 | 0.98 | 1.23 | 1.01 | 1.24 | 0.87 | 0.79 |
| -0.12 | -0.08 | 0.02 | 0.01 | 0.00 | -0.01 | 0.03 | 0.04 | 0.03 | 0.00 | 0.02 | 0.03 | 0.04 | -0.03 | -0.07 |
| 0.70 | 1.22 | 0.96 | 1.22 | 1.01 | 1.23 | 0.99 | 1.19 | 0.98 | 1.23 | 1.02 | 1.24 | 0.98 | 1.25 | 0.72 |
| -0.01 | 0.01 | 0.02 | 0.02 | -0.02 | 0.00 | 0.00 | 0.02 | 0.00 | 0.00 | -0.01 | 0.02 | 0.03 | 0.02 | 0.03 |
| 0.57 | 0.86 | 1.28 | 1.03 | 1.27 | 1.02 | 1.24 | 1.01 | 1.24 | 1.02 | 1.28 | 1.05 | 1.31 | 0.88 | 0.58 |
| 0.18 | 0.00 | -0.04 | -0.08 | -0.04 | -0.01 | 0.02 | 0.01 | 0.02 | 0.00 | -0.05 | -0.11 | -0.08 | -0.03 | 0.19 |
| | 0.83 | 1.07 | 1.21 | 1.03 | 1.24 | 1.02 | 1.24 | 1.02 | 1.25 | 1.05 | 1.24 | 1.11 | 0.86 | |
| | 0.00 | -0.12 | -0.22 | -0.07 | 0.03 | 0.03 | 0.05 | 0.05 | 0.04 | -0.09 | -0.29 | -0.20 | -0.09 | |
| | 0.62 | 0.75 | 1.08 | 1.30 | 0.99 | 1.25 | 1.00 | 1.26 | 1.00 | 1.33 | 1.12 | 0.79 | 0.65 | |
| | 0.11 | -0.03 | -0.11 | -0.03 | 0.04 | 0.03 | 0.03 | 0.05 | 0.06 | -0.04 | -0.17 | -0.11 | 0.01 | |
| | | 0.63 | 0.84 | 0.88 | 1.26 | 0.88 | 1.32 | 0.89 | 1.29 | 0.91 | 0.87 | 0.66 | | |
| | | 0.11 | 0.00 | 0.02 | 0.02 | -0.05 | -0.05 | -0.02 | 0.06 | 0.02 | -0.04 | 0.03 | | |
| | | | | 0.58 | 0.73 | 0.80 | 0.80 | 0.81 | 0.75 | 0.60 | | | | |
| | | | | 0.18 | 0.01 | -0.10 | -0.10 | -0.07 | 0.07 | 0.24 | | | | |

**Fig. 19.** Changes of monitored detector responses by monitored power feedback.

is hit. Detector measurements are then taken as the detectors being pulled back through the core at a constant speed. If a detector was failed, measurements should be similar with the shape of channel "H11" as shown in Fig. 15. Measurements as shown in Fig. 14 might be an incident or other unknown operation phenomenon. But in this paper, both measurements like channel of " H15"/"G09" in Fig. 14 and measurements like channel "H11" in Fig. 15 were considered as the detector failure. As the function of diagnosis of the detector failure has been implemented in NECP-ONION, the monitoring calculation was performed again by removing failed detector readings. As the result, relative errors of radial-average detector responses decrease slightly as shown in Fig. 16.

Secondly, it is observed that it is difficult to simulate real-world detector responses because of the complex operation history, unknown control rod positions, and unexpected radial tilts of the detector measurements for the BEAVRS benchmark problem. Specifically, the unexpected radial tilt of detector measurements at BOC, caused by some unidentified operation events, cannot be modeled directly in the simulation.

Because detector measurements are the real reflection of the core operation states, two improvements for on-line monitoring have been studied to increase the monitoring accuracy of the NECP-ONION system as follows.

Due to the complex operation history, unknown control rod position, unidentified operation events, approximation of the diffusion solver, the calculation of core burnup distribution based on the diffusion-based power distribution was not necessarily the reflection of the real distribution. Hence the first improvement is to use the monitored power distribution instead of the diffusion-based power distribution to calculate the burnup distribution more realistically. As the power distribution and burnup distribution affect each other, the accuracy of on-line monitoring will be improved with this new approach. Taking the second monitored points as an example, the corresponding burnup distribution, power distribution, and monitored detector responses are shown in Figs. 17–19, respectively. Burnup and power distribution changed greatly but monitored detector responses changed slightly. It demonstrates that the monitoring accuracy improves slightly as shown in Fig. 20. The second improvement is to use the monitored power distribution of the last step as the fundamental mode. On one hand, the radial tilt of detector measurements is part of the reasons for the monitoring error. Hence the use of the fundamental mode reflecting such tilt would improve the monitoring accuracy. On the other hand, use of the most recent monitored power distribution as the fundamental mode is benefit for the monitoring system to capture core characteristics caused by operation events which cannot be modeled by the diffusion calculation. Similarly, slight improvement is observed by this method as shown in Fig. 21.

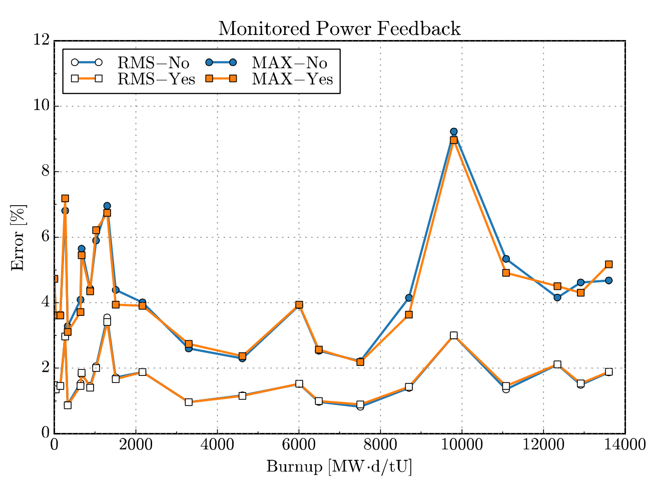


**Fig. 20.** Relative errors of radial-average detector responses with monitored power feedback.

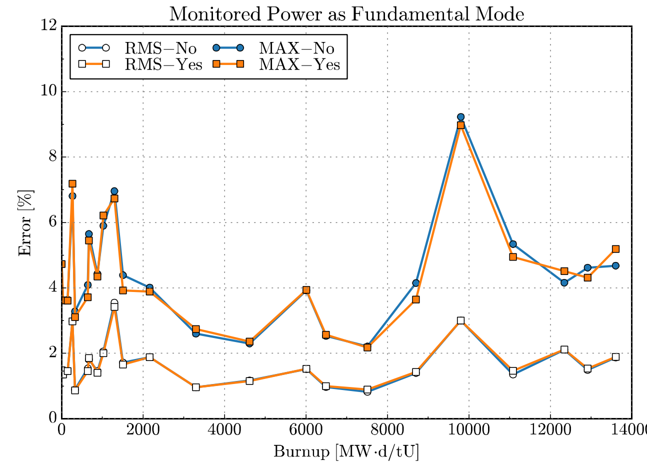


**Fig. 21.** Relative errors of radial-average detector responses with employment of monitoring experience.

## 4. Conclusions

A 3D on-line power-distribution monitoring system, NECP-ONION, has been developed. It includes plant data processing, core calculation and on-line power-distribution monitoring. The diagnosis and treatment of the detector failure, core state-parameter calculation and monitoring method has been investigated to address the key issues of the on-line monitoring system. Detector failure is diagnosed by comparison with average measurements and monitored responses. The fuel-burnup calculation is performed based on the macro-depletion method due to its efficiency. The harmonics expansion method is adopted as the major monitoring method due to its long history of maturity and success. In the investigation of the harmonics expansion method, the determination of expansion orders and choice of expansion basis functions have also been studied.

The on-line monitoring system NECP-ONION was verified and validated by the diffusion calculation and real detector measurements for the BEAVRS benchmark. Before comparing with the plant measurements, the verification was carried out by comparing NECP-ONION monitoring results with those of the diffusion calculation to assess the faithfulness of the on-line monitoring system against the conceptual design of the NECP-ONION system. The verification shows that, for BEAVRS cycle 1 with a complex power history, the monitoring power distributions are almost identical to the reference power distributions once the detector "measurements" are derived from the diffusion calculation.

Detector measurements provided in the BEAVRS benchmark problem were then used to validate NECP-ONION. The validation shows that differences between monitored and measured ones are small for most of the burnup steps, except for few abnormal discrepancies at specific burnup steps. Investigation shows that those discrepancies are caused by the detector failure, complex operation history, unknown control rod positions, and unidentified operation events which cannot be modeled directly in the simulation. Based on the investigation, two improvements were proposed to increase the monitoring accuracy of the NECP-ONION system. The first improvement is to use the monitored power distribution instead of the diffusion-based power distribution to calculate the burnup distribution more realistically. The second improvement is to use the most recent monitored power distribution as the fundamental mode to capture core characteristics caused by operation events which cannot be modeled by the diffusion calculation. Numerical results indicate that both of these two improvements help to increase the monitoring accuracy for the BEAVRS benchmark. Furthermore, the uncertainty of the nuclear cross-section data will be propagated to the monitoring results. This will be a very important topic of the future work.

## Acknowledgements

This research was financially supported by the National Natural Science Foundation of China (No. 11305123).

## References

Beard, C., Morita, T., 1988. The BEACON core monitoring system. Trans. Am. Nucl. Soc. 56, 518–519.

Chan, P.S.W., Mamourian, M., April 18–20, 1990. Application of on-line solution of 3-dimensional multigroup finite-difference neutron diffusion equations in reactor power control system. In: Third International Conference on Simulation method in Nuclear Engineering. Montreal, Quebec.

Hinchley, E., Kugler, G., October, 1974. On-line control of the CANDU-PHWR power distribution. In: IAEA Specialists Meeting on Spatial Control Problems, Studsvik, Sweden.

Hong, I.S., 2004. Flux Mapping Methods for CANDU Reactors Based on Least Squares Principle and Error Shape Synthesis (Ph.D. thesis). Seoul National University, Seoul, Korea.

Hong, I.S., Kim, C.H., Suk, H.C., 2005. Advanced online flux mapping of CANDU PHWR by least-squares method. Nucl. Sci. Eng. 150, 299–309.

Horelik, N., Herman, B., 2013. MIT Benchmark for Evaluation and Validation of Reactor Simulations. MIT Computational Reactor Physics Group. Rev. 1.1.1.

Horelik, N., Herman, B., Forger, B., et al., 2013. Benchmark for evaluation and validation of reactor simulations (BEAVRS), M&C 2013, Sun Valley, Idaho.

Jeong, C.J., Cho, N.Z., 2000. Power mapping in a Canada deuterium uranium reactor using Kalman filtering technique. J. Nucl. Sci. Technol. 37, 758–768.

Jeong, W.S., Lee, H.C., Kim, H.S., et al., 2014. Development of online core monitoring methodology applying periodic 3DPCM for KSNP. Trans. Am. Nucl. Soc.

Kelly, D.J., Aviles, B.N., Romano, P.K., et al., 2014. Analysis of select BEAVRS PWR benchmark cycle 1 results using MC21 and OpenMC, PHYSOR, Kyoto, Japan.

Lee, K.B., Kim, C.H., 2003. The least-squares method for three-dimensional core power distribution monitoring in pressurized water reactors. Nucl. Sci. Eng. 143, 268–280.

Lehoucq, R.B., Sorensen, D.C., Yang, C., 1997. ARPACK Users' Guide: Solution of Large-Scale Eigenvalue Problems with Implicitly Restarted Arnoldi Methods. Rice University.

Li, F., 1994. Harmonics Synthesis Method for Core Flux Distribution Reconstruction and its Application to Diagnosis (Ph.D. thesis). Tsinghua University, Beijing, China (In Chinese).

Li, F., Luo, Z., Hu, Y., 1997. Harmonics synthesis method for core flux distribution reconstruction. Prog. Nucl. Energy 31, 369–372.

Li, Z., Wu, H., Cao, L., et al., May 17–22, 2015. 3D PWR power distribution on-line monitoring based on harmonics expansion, ICONE-23, Chiba, Japan.

Li, Z., Wu, H., Cao, L., et al., August 23–26, 2016. Diagnosis and processing of detector failure in PWR on-line power distribution monitoring, CORPHY 2016, Beijing, China. (In Chinese).

Li, Y., Yang, W., Wu, H., et al., 2016b. NECP-Cypress: Development and Benchmarking of a 3D PWR Core-Analysis Code. Transaction of the American Nuclear Society, New Orleans, LA, USA. June 12–16.

Li, Z., Wu, H., Cao, L., et al., May 1–5, 2016. On-line monitoring analysis of BEAVRS benchmark using NECP-ONION, PHYSOR2016, Sun Valley, Idaho, USA.

Liao, C., 2002. Study on Numerical Method for Three Dimensional Nodal Space-Time Neutron Kinetic Equations and Coupled Neutronic/Thermal-Hydraulic Core Transient Analysis. Xi'an Jiaotong University, Xi'an, China (Ph.D. thesis), (In Chinese).

Luo, Z., Li, F., Wang, Y., et al., 2000. An idea about applying the online surveillance techniques to safe reactor operation. Chin. J. Nucl. Sci. Eng. 20, 32–38 (In Chinese).

Mishra, A.K., Shimjith, S.R., Bhatt, T.U., et al., 2014. Kalman filter-based dynamic compensator for Vanadium self powered neutron detectors. Trans. Nucl. Sci. 61, 1360–1368.

Peng, X., Wang, K., Li, Q., 2014. A new power mapping method based on ordinary Kriging and determination of optimal detector location strategy. Ann. Nucl. Energy 68, 118–123.

Shen, W., Schwanke, P., 2012. Evolution of RFSP 3.5 for CANDU analysis. In: Proc. of the 33rd Canadian Nuclear Society (CNS) Annual Conference, Saskatoon, Saskatchewan, Canada, June 10-13.

Terney, W.B., Biffer, J.L., Dechand, C.O., et al., 1983. The C-E CECOR fixed in-core detector analysis system. Trans. Am. Nucl. Soc. 44, 542–543.

Verdu, G., Miro, R., Ginestar, D., et al., 1999. The implicit restarted Arnoldi method, an efficient alternative to solve the neutron diffusion equation. Ann. Nucl. Energy 26, 579–593.

Wang, C., Wu, H., Cao, L., et al., 2011. On-line reconstruction of in-core power distribution by harmonics expansion method. Nucl. Eng. Des. 241, 3042–3050.

Zinzani, F., Demaziere, C., Sunde, C., 2008. Calculation of the eigenfunctions of the two-group neutron diffusion equation and application to modal decomposition of BWR instabilities. Ann. Nucl. Energy 35, 2109–2125.